An experimental set-up for carbon isotopic analysis of atmospheric CO_2 and an example of ecosystem response during solar eclipse 2010

Tania Guha and Prosenjit Ghosh*

Centre for Earth Sciences, Indian Institute of Science, Bangalore 560 012, India.
**Corresponding author. e-mail: pghosh@ceas.iisc.ernet.in*

We present here, an experimental set-up developed for the first time in India for the determination of mixing ratio and carbon isotopic ratio of air-CO_2. The set-up includes traps for collection and extraction of CO_2 from air samples using cryogenic procedures, followed by the measurement of CO_2 mixing ratio using an MKS Baratron gauge and analysis of isotopic ratios using the dual inlet peripheral of a high sensitivity isotope ratio mass spectrometer (IRMS) MAT 253. The internal reproducibility (precision) for the $\delta^{13}C$ measurement is established based on repeat analyses of $CO_2 \pm 0.03‰$. The set-up is calibrated with international carbonate and air-CO_2 standards. An in-house air-CO_2 mixture, 'OASIS AIRMIX' is prepared mixing CO_2 from a high purity cylinder with O_2 and N_2 and an aliquot of this mixture is routinely analyzed together with the air samples. The external reproducibility for the measurement of the CO_2 mixing ratio and carbon isotopic ratios are ± 7 ($n = 169$) $\mu mol \cdot mol^{-1}$ and ± 0.05 ($n = 169$) ‰ based on the mean of the difference between two aliquots of reference air mixture analyzed during daily operation carried out during November 2009–December 2011. The correction due to the isobaric interference of N_2O on air-CO_2 samples is determined separately by analyzing mixture of CO_2 (of known isotopic composition) and N_2O in varying proportions. A $+0.2‰$ correction in the $\delta^{13}C$ value for a N_2O concentration of 329 ppb is determined. As an application, we present results from an experiment conducted during solar eclipse of 2010. The isotopic ratio in CO_2 and the carbon dioxide mixing ratio in the air samples collected during the event are different from neighbouring samples, suggesting the role of atmospheric inversion in trapping the emitted CO_2 from the urban atmosphere during the eclipse.

1. Introduction

Carbon isotope ratios and CO_2 mixing ratios ($\mu mol \cdot mol^{-1}$) in air are the fundamental parameters used for estimating the fluxes of CO_2 from different sources or sinks, e.g., oceanic, biospheric and anthropogenic (Hoefs 1995). The method of simultaneous monitoring of carbon isotope ratio and concentration of CO_2 for such a purpose was established during the 1960's (Keeling 1958) but gathered momentum in the last two decades, on the realization of the importance of CO_2 on climate change and subsequently global network of CO_2 monitoring stations was established worldwide (Tans *et al.* 1990). Several factors hindered the progress in air-CO_2 isotope based research. These include developing complicated analytical protocols for air sampling, quantitative extraction of CO_2 from air and accurate mass spectrometric analyses of isotopic ratios following the scaling of the isotopic ratio to the VPDB scale through primary reference material (like NBS19) and finally the intercomparison of data between different laboratories to merge the data for better understanding

Keywords. Air-CO_2; isotope measurement; dual inlet; IRMS; mass spectrometry.

the global CO_2 flux (Toru and Kazuto 2003). Both the CLASSIC (Circulation of Laboratory Air Standards for Stable Isotope intercomparisons) cylinder experiment conducted by CSIRO (Allison *et al.* 2002; Toru and Kazuto 2003) and the NOAA/CSIRO flask air intercomparison experiment (Masarie *et al.* 2001) provided comprehensive understanding of the factors driving the analytical uncertainty of air-CO_2 measurement, i.e., both for cylinder and flask air analyzed at different laboratories around the world. The factors crucial for achieving better precision include monitoring the isotope ratios of reference air mixture for routine check, comparison with International standard with known air-CO_2 composition and NBS19-CO_2 in air standards for calibration. To further improve the link of air-CO_2 to primary reference standard, generation of high purity CO_2 from carbonate standard with high precision and mixing with CO_2-free air is necessary (Toru and Kazuto 2003). This was achieved at MPI-BGC Jena through accurately preparing CO_2 from carbonate standards and mixing it in a cylinder with CO_2-free air (Jena Reference Air Set, JRAS) using a fully automated system (Ghosh *et al.* 2005; Laurila 2007; Wendeberg *et al.* 2011). A set of JRAS reference air allows intercomparison of the data produced in different laboratories through an analysis of a common reference flask air and the determination of the local scale offset from the international scale.

An important requirement in air-CO_2 isotope research is the design of an experimental apparatus for air-CO_2 extraction and purification using cryogenic protocol. The procedure should demonstrate a consistent yield of CO_2, minimize the interaction of CO_2 and water, and reproduce isotopic composition from the same air samples while processing air samples from the flask involving cryogenic procedures. The performance can be monitored with analyses of an aliquot of air from an air-CO_2 reference cylinder. The method of cryogenic separation of CO_2 from air samples cannot prevent the simultaneous condensation of N_2O with CO_2, which introduces isobaric interference in the $\delta^{13}C$ ratio determination during mass spectrometric analyses (Mook and Hoek 1983). A correction factor for the N_2O contribution is required (Mook and Hoek 1983) and has been determined in the present study by a separate experiment.

We present here initial results and some observations from an experimental set-up intended to deliver high precision isotopic ratio in air-CO_2. Using the experimental set-up, the mixing ratio and $\delta^{13}C$ variability of air-CO_2 during the annular solar eclipse day of 15 January, 2010 were observed.

2. Experimental details

2.1 *Sample collection*

Air sample collection is done in Pyrex flasks of 1 litre capacity with a stopcock following a design developed by CSIRO, Australia (Francey *et al.* 1996). While sampling, a pair of flasks are placed in a compartment inside an aluminum metal box. An arrangement of valves, traps and an analog pressure gauge are positioned within the box to allow filling of air in the glass flasks at a final pressure of 1.2 bar. A Magnesium perchlorate [$Mg(ClO_4)_2$] trap is used to get rid of moisture. Electro-polished stainless steel (SS) tubing is used in the sampler to reduce the surface adsorption of gases. Other features include needle valves for releasing excess pressure (above 1.2 bar) in the flask (figure 1a). These components are connected through Swagelok union fittings and an external pump (NMP 850 KNDC. KNF Neuberger, Freiburg, Germany) is used for filling air in the flasks. The sample collection procedure involves initial flushing of the line with ambient air for a period of 10 minutes. A flow rate of ∼4.5 l/min is measured at the outlet during the operation. Finally, the flasks are filled with air and pressurized for a period of ∼5 min until a pressure of ∼1.2 bar is attained. The flasks are disconnected from the unit and kept ready for extraction and analyses.

2.2 *Extraction of CO_2 from air sample*

CO_2 is extracted from the air sample by a cryogenic procedure (Craig 1953) in a stainless steel extraction line, called the Trap box following a prototype, in operation at MPI, Jena (Werner *et al.* 2001). The set-up is manually operated using a set of Swagelok needle valves. The Trap box is fitted with a mass flow controller (flow rate 10–100 ml/min) (MKS Instruments, Andover, USA) to regulate the flow through two traps (one dole trap and one U-trap) in a series (figure 1b). The mass flow controller and the traps are connected via Swagelok union fittings. The input of the dole trap is connected with the mass flow controller and the output to a U-trap. In a sequence, the outlet of the U-trap can either be connected to a membrane pump or to a Turbo molecular pump (http://www.pfeiffer-vacuum.com/) via a cold trap. The membrane pump is used for withdrawal of air from the flask; air is allowed to expand and flow through the traps where along with CO_2 other condensable gases are trapped at liquid nitrogen temperature (−196°C). During the trapping operation, the pressure in the line is maintained at ∼25 mbar; this is necessary to minimize the possibility of trapping contaminants like oxygen

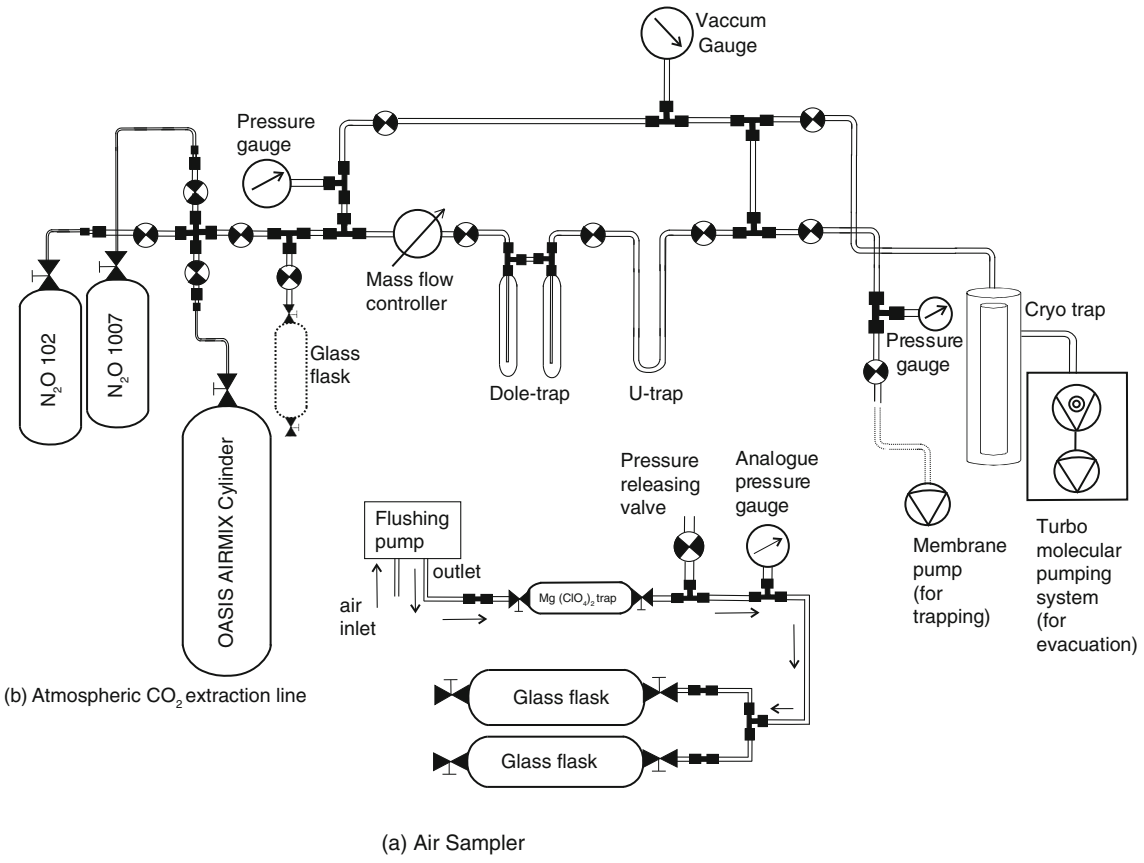

Figure 1. Schematic diagram showing layout of the (**a**) air sampler and (**b**) air-CO_2 extraction line used for the collection and extraction of CO_2 from the air sample for mixing ratio and isotope ratio determination.

and argon (Werner *et al.* 2001). A flow rate of 100 ml/min is maintained using the mass flow controller. Ethanol slurry held at −80°C is used for the efficient trapping of water vapour, present in the air sample. During the purification stage, CO_2 ($+N_2O$) is slowly distilled by altering the temperature of the trap from −196°C to −80°C and the mixture is finally transferred into a sample finger with known volume, fitted with a stop cock. Determination of finger volume is done gravimetrically knowing the weight of empty ampoule and the ampoule filled (up to the brim) with water. The difference of these weights and the density of distilled water (0.9977 gm/cc at 22°C) allow determination of finger volume, which was 2.6 ± 0.1 ml as estimated. The sampling finger used for collection of CO_2 remained same throughout the period of our experiment.

2.3 *Measurement of mixing ratio and $\delta^{13}C$ of the extracted CO_2*

The CO_2 extracted in the sample tube is expanded to a fixed volume (15 ± 0.1 ml) of the extraction set-up and the corresponding pressure recorded at the digital display unit of MKS Baratron Gauge is converted into the micromoles of CO_2 at room temperature, using the pressure-volume relationship. Two known volumes (as ampoules) were used, where a fixed amount of CO_2 was expanded using cryogenic method to determine the line volume (referred as fixed volume). A typical pressure reading obtained during air sample extraction is ∼30 mbar. Using these parameters in the pressure volume relation of the ideal gas law ($pV = nRT$), where p is the pressure measured using the MKS Baratron gauge, V is the fixed volume determined and T is the average temperature of 30°C maintained at our laboratory, we obtained micromoles of the extracted CO_2. The mixing ratio of air-CO_2 ($\mu mol \cdot mol^{-1}$) is established based on the knowledge of the volume of air processed from the glass flask (Affek and Eiler 2006), initial flask pressure at constant temperature and the micromole of CO_2 retrieved from unit volume of air processed during the experiment.

The CO_2 from the air is transferred into a glass finger and later fed into the Dual inlet (DI) peripheral of a Finnigan-MAT 253 isotope ratio mass spectrometer (Thermo-Fisher, Bremen, Germany). In the mass spectrometer, the molecular ion currents at mass-to-charge ratios (m/z) of 44, 45 and 46 are measured to derive the elemental isotope ratios, i.e., $^{13}C/^{12}C$ and $^{18}O/^{16}O$, relative to a

working gas/reference CO_2. The $\delta^{13}C$ values are also corrected for the ^{17}O contribution based on the ^{18}O signal measured in the sample (Santrock *et al.* 1985). The isotopic ratios are expressed in δ-notation which is defined as:

$$\delta = (R_{sample}/R_{standard} - 1)$$

where $R = {}^{13}C/{}^{12}C$. δ values are expressed in ‰.

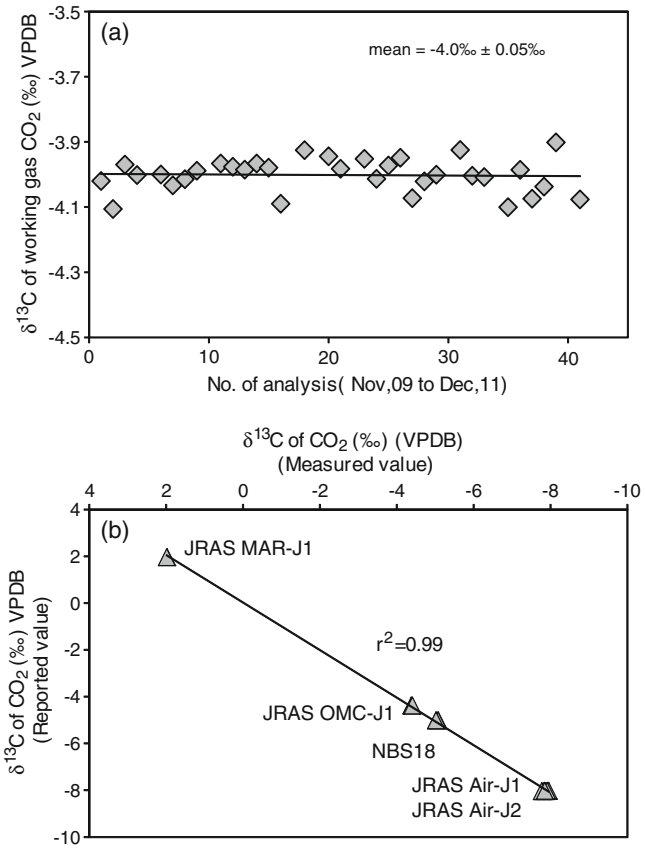

Figure 2. (**a**) Time variation of the working gas isotopic composition measured relative to the CO_2 generated from carbonate standards NBS19 and MARJ1, (**b**) linear behaviour of mass spectrometric analyses involving different standards, including carbonates standard NBS18 and JRAS MAR-J1, JRAS OMC-J1, JRAS Air-J1 and JRAS Air-J2 reference mixture.

The internal precision for the $\delta^{13}C$ measurement in the IRMS MAT253 is ±0.03‰ for a sample size of 15–20 µmol of CO_2, measured at a major beam voltage of 3–4 V. This internal precision is established based on two replicate measurements (each measurement consists of 10 alternative introduction of CO_2 from the reference and the samples side of the changeover valve) of Linde high purity CO_2, which is used as the working gas for our measurement. The procedure for analysis involves calibration of the working gas and assigning values relative to VPDB. The experimental procedure involves the reaction of carbonate powders with 105% phosphoric acid at 25°C in a McCrea type reaction vessel for 18 hours (McCrea 1950; Ghosh *et al.* 2005) and the CO_2 produced after the reaction is cryogenically separated and analyzed relative to the working gas. Carbonate standards NBS19 and MARJ1 were used for the assignment of value to the working gas on the VPDB scale (Ghosh *et al.* 2005). The procedure was repeated regularly at monthly intervals to monitor the variation of the working gas composition with time (displayed in figure 2a) and to understand long term reproducibility of primary standard. The long term (23 repeat analyses) precision for the NBS19 analysis was ±0.03‰. NBS18 was also analyzed on few occasions and the $\delta^{13}C$ value observed was −5.05 ± 0.03‰, which lie close to IAEA (International Atomic Energy Agency) recommended values (Stichler 1995; Coplen 1996) (table 1). During the cryogenic separation of air, experimental effects like trapping efficiency, fractionation upon thawing, co-trapping of traces of air, etc., cause errors in isotopic measurement, compared to a measurement done on CO_2 from a high purity cylinder (Werner *et al.* 2001). To address this issue, there was a suggestion to analyse simultaneously an aliquot of air from an air-CO_2 mixture (treated as a reference cylinder) following the identical preparation steps adopted for the samples (Laurila 2007). To express the delta values of the air-CO_2 samples in VPDB scale, a set of JRAS

Table 1. *Analysis of JRAS MAR-J1, JRAS OMC-J1 and primary carbonate standards NBS19 and NBS18.*

Standard run	Number of run	Mixing ratio (µmol·mol^{-1})	Assigned value for mixing ratio (µmol·mol^{-1})	Offset# for mixing ratio (µmol·mol^{-1})	$\delta^{13}C$* (‰ VPDB)	Assigned value for $\delta^{13}C$ (‰ VPDB)	Offset# for $\delta^{13}C$ (‰ VPDB)
International carbonate standard							
NBS19	23	–	–	–	1.95 ± 0.03	–	–
NBS18	3	–	–	–	−5.05 ± 0.03		
International air standard							
JRAS MAR-J1	2	362.3 ± 2	362	0.3	1.98 ± 0.01	1.96	0.02
JRAS OMC-J1	3	356.8 ± 2	357	−0.2	−4.39 ± 0.02	−4.38	−0.01

*: NBS-19 −CO_2 is used as anchor to define the composition of working gas.
#: Offset = local scale value − assigned value.

reference air mixture, i.e., JRAS MAR-J1 and JRAS OMC-J1 (table 1) provided by MPI, BGC are used (http://www.bgc.mpg.de/service/iso_gas_lab/JRAS_web/). Two separate air mixture glass flasks with $\delta^{13}C$ values (JRAS Air-J1: $\delta^{13}C = -8.04‰$ and JRAS Air-J2: $\delta^{13}C = -8.02‰$) close to air are supplied from MPI for testing the extraction protocol. To address the linearity in the delta scale, $\delta^{13}C$ values of these standards (4 JRAS reference flasks and NBS18 analysis) are plotted against the recommended values (referred as literature values) (figure 2b).

2.4 *Determination of N_2O correction factor for $\delta^{13}C$ of air-CO_2*

N_2O behaves like CO_2 during cryogenic separation and introduces isobaric interference during the determination of isotopic ratios in air-CO_2 samples (Mook and Groots 1973). To obtain the correct $\delta^{13}C$ value for air-CO_2, it is important to introduce a correction factor for the N_2O contribution (Mook and Hoek 1983; Ghosh and Brand 2004). The determination of the correction factor for the N_2O contribution involves measurement of the ionization efficiency of N_2O in IRMS, which is instrument specific. The ionization efficiency of pure N_2O drastically differs from the ionization efficiency of the $N_2O + CO_2$ mixture (Craig and Keeling 1963). As a result, individual laboratories involved with air-CO_2 measurements establish their own scheme to correct for the presence of N_2O in the air-CO_2 sample. To determine the N_2O correction factor two high pressure LUXFER cylinders (http://www.luxfercylinders.com/) (10 l in volume) with different mixing ratios of CO_2 and N_2O (Chemix Speciality Gases and Equipment, Bangalore) are used. The composition of gases in the individual cylinders are: cylinder 1 contain 1007 ppb N_2O, 370 ppm CO_2, 20.6% O_2, balanced with N_2 and is referred to as 'N_2O 1007' and cylinder 2 is composed of 102 ppb N_2O, 388 ppm CO_2, 20.2% O_2, balanced with N_2 and is referred to as 'N_2O 100'. The CO_2 added in both the cylinders originates from the same Linde CO_2 tank, which is used as the CO_2 working gas. The cylinders are connected with the trap box using an arrangement shown in figure 1(b). The $\delta^{13}C$ values of CO_2

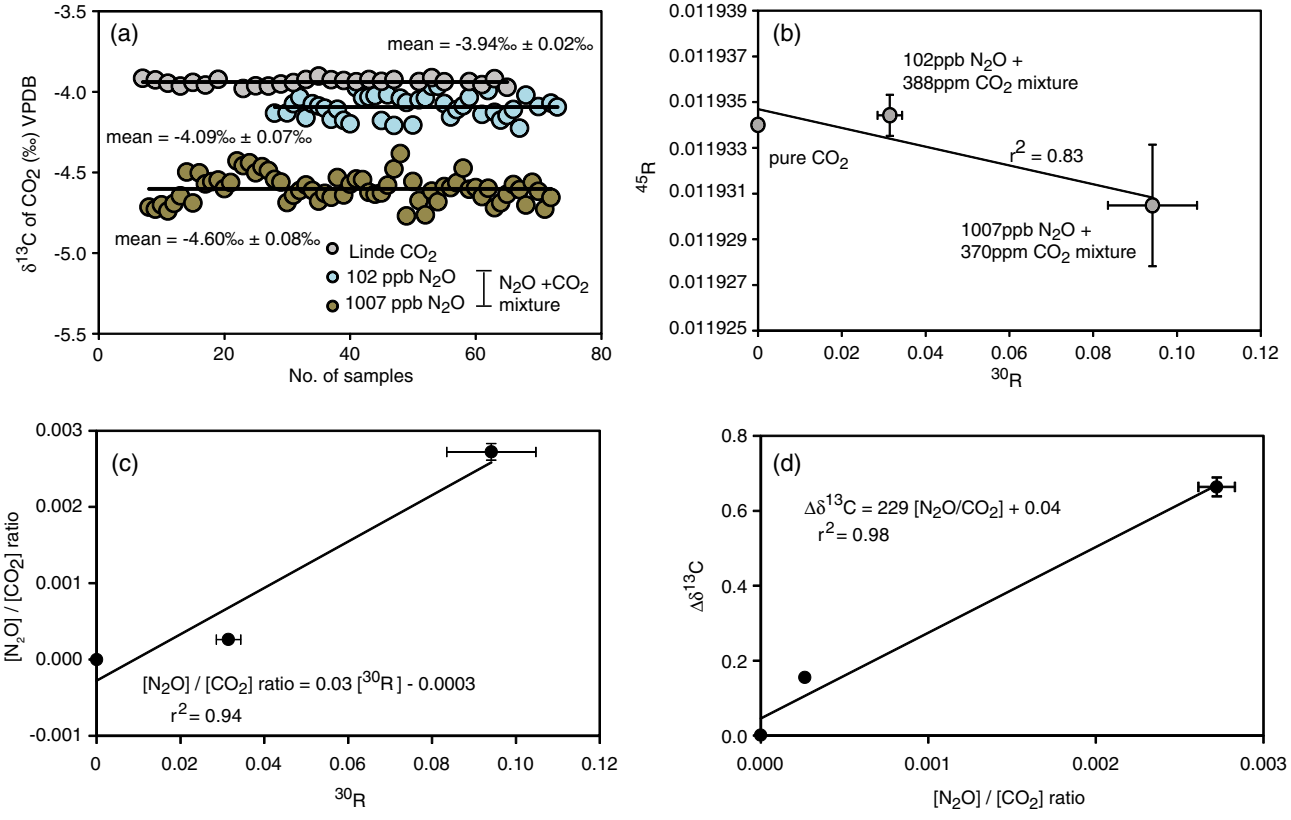

Figure 3. (**a**) The variation in the $\delta^{13}C$ values for CO_2 due to isobaric interference of N_2O based on delta values of air mixture with 1007 ppb N_2O (CO_2 concentration of 393 ppm) and comparison with two other air mixture with 102 ppb N_2O (CO_2 concentration of 407 ppm) and without any N_2O, i.e., Linde CO_2, (**b**) correlation between ^{45}R and ^{30}R of N_2O–CO_2 mixture suggesting change in ^{30}R as measure of N_2O/CO_2 ratio in the samples, (**c**) a linear relationship used for the determination of N_2O/CO_2 ratio from ^{30}R mass intensity and (**d**) a linear relationship between the $\delta^{13}C$ offset ($\Delta\delta^{13}C$) or correction factor and N_2O/CO_2 ratio. Error bars shown in the plots represent uncertainty in repeat measurement.

extracted from the Linde CO_2, the 'N_2O 1007' and the 'N_2O 102' cylinders are plotted in figure 3(a). The $\delta^{13}C$ value obtained for 'N_2O 1007', 'N_2O 102' cylinders and Linde CO_2 are -4.60 ± 0.08‰, -4.09 ± 0.07‰ and -3.94 ± 0.02‰, respectively. The difference ($\Delta\delta^{13}C$) between the $\delta^{13}C$ value of Linde CO_2 and CO_2 extracted from respective cylinders, i.e., 'N_2O 1007' and 'N_2O 102' cylinders is attributed to the N_2O contribution. The relationship obtained between $\Delta\delta^{13}C$ and the N_2O concentration is used for deriving the correction factor for the N_2O contribution. The N_2O/CO_2 ratio is determined by measuring the ^{30}R mass intensity of the extracted CO_2 from the respective cylinders. During the mass spectrometric analysis, both the ^{45}R and ^{30}R intensities are determined where, $^{45}R = {}^{45}I/{}^{44}I$ and $^{30}R = {}^{30}I/{}^{44}I$, I denotes ratio of ion beam intensity and the ^{30}R and ^{45}R values are corrected for the ^{17}O contribution. The ^{30}R is a product of the dissociation of CO_2 and N_2O ($N^{14}O^{16}$ and $C^{12}O^{18}$) (Assonov and Brenninkmeijer 2006) and it is used to determine the $[N_2O]/[CO_2]$ ratio in the sample. The procedure followed is described in Assonov and Brenninkmeijer (2006), and the ^{30}R value is found to correlate linearly with ^{45}R value for the mixture with different N_2O/CO_2 ratios in them, as given in figure 3(b). Thus changes in both ^{45}R and in ^{30}R are equally proportional to the amount of N_2O present in a mixture. This suggests the use of ^{30}R as a measure for $[N_2O]/[CO_2]$ ratios in air samples. A linear relationship between N_2O/CO_2 ratio and ^{30}R mass intensity (figure 3c) allows the determination of N_2O concentration in the air samples by knowing the ^{30}R beam intensity. Further, a linear relationship between $\Delta\delta^{13}C$ and the N_2O/CO_2 ratio (figure 3d) provides the correction factor for a particular ratio of N_2O/CO_2. The correction factor introduced for the $\delta^{13}C$ measurement for air-CO_2 was +0.2‰ at 329 ppb of N_2O content. The variable $[N_2O]/[CO_2]$ ratios of the cylinder air allowed defining the slope of a linear regression. The uncertainty in the slope of the two linear equations (calculated using LINEST function in Excel 2007) displayed in figure 3(c and d) respectively lead to an error of ±0.07‰ in the correction factor determination for $\delta^{13}C$ of air-CO_2 (www.physics.arizona.edu/physics/). This error when added quadratically with the air-CO_2 sample error gives rise to a final error of ±0.08‰ for $\delta^{13}C$ measurement of air samples.

2.5 *Validation of the calibration of the working gas using JRAS air reference*

To firmly link our air-CO_2 measurement to the VPDB scale, JRAS reference air samples, JRAS MAR-J1 (assigned $\delta^{13}C$ value of 1.96‰) and JRAS OMC-J1 (assigned $\delta^{13}C$ value of −4.38‰) (http://www.bgc.mpg.de/service/iso_gas_lab/JRAS_web/) (Laurila 2007) procured from Isolab, Max Plank Institute, Jena are analyzed. The reference mixture in 5 l volume glass flask at 1.2 bar pressure is extracted for three times (1 litre splits) and analyzed for its CO_2 mixing ratio and $\delta^{13}C$. The JRAS air reference is first introduced into the DI peripheral and measured for isotope ratios w. r. t. the Linde CO_2 as the working gas. Then the $\delta^{13}C$ value of JRAS air-CO_2 is determined in the VPDB scale using simultaneous measurements of CO_2 from reacting primary carbonate standards, i.e., NBS19. This $\delta^{13}C$ value is designated as the local scale value for the JRAS air reference. The set of JRAS reference air samples have assigned values for both the mixing ratio and the $\delta^{13}C$ of CO_2, i.e., JRAS MAR-J1 (mixing ratio = 362 μmol·mol^{-1} and $\delta^{13}C$ = 1.96‰) and JRAS OMC-J1 (mixing ratio = 357 μmol·mol^{-1} and $\delta^{13}C = -4.38$‰). The difference between the local scale value and the assigned value for the JRAS reference is defined as a scale offset. The pair of JRAS reference air, i.e., MAR-JI air and OMC-J1 yield an offset value of +0.3 μmol·mol^{-1} and −0.2 μmol·mol^{-1}, respectively for the mixing ratio. The offset for the $\delta^{13}C$ of CO_2 analyzed from them are +0.02‰

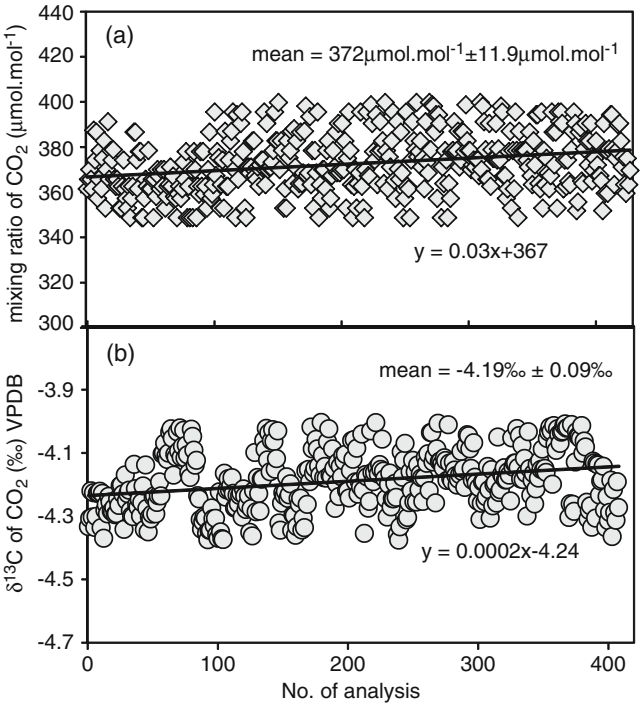

Figure 4. Time bound variation of (**a**) the mixing ratio and (**b**) the $\delta^{13}C$ of air-CO_2 extracted from the OASIS AIRMIX cylinder used as internal air reference mixture. The long term mean and standard deviation of measurement are mentioned in the figure along with drift (based on alternate day measurements).

Table 2. *Reproducibility of internal air reference material and atmospheric samples.*

Standard run	Number of run	Mixing ratio (μmol·mol^{-1})	$\delta^{13}C^*$ (‰ VPDB)
Internal air reference: OASIS AIRMIX			
External reproducibility*	–	7	0.05
Long term reproducibility#	418	±12	±0.09
Atmospheric air samples collected at the same time			
External reproducibility*	–	7	0.05

*: Mean of the differences (total number of such differences is 169) between the two measurements performed in a day on paired sample.
#: Standard deviation of all the 418 samples extracted and analysed during this period.

and −0.01‰, respectively. The average values for both mixing ratios and $\delta^{13}C$ are 0.05 μmol·mol^{-1} and 0.005‰, respectively (table 1). These offsets are incorporated in the $\delta^{13}C$ measurement of air-CO_2 analyzed using our experimental set-up. The reproducibility (standard deviation) of the repeat extraction and measurements (3 times) of JRAS reference air for mixing ratio, $\delta^{13}C$ is ±2 μmol·mol^{-1}, ±0.02‰, respectively, as mentioned in table 1.

2.6 *Internal air reference material*

The long term reproducibility of an experimental set-up requires consistent monitoring through repeated analyses of the synthetic air-CO_2 mixture with only CO_2, O_2 and N_2. One such mixture, OASIS AIRMIX is prepared in a 40 l pressurized cylinder (120 psig) mixing oxygen (20.4%), CO_2 (401 ppm) and balanced with residual N_2. The cylinder was prepared under our supervision at Bhoruka Gases Ltd., Bangalore using Linde high purity CO_2, which is used as the working gas. An aliquot of the OASIS AIRMX is processed routinely together with our air samples. The isotopic ratios of CO_2 and concentration are routinely measured for the air samples during the air-CO_2 experiment. The cylinder is connected to the line with a stainless steel regulator (http://www.indiamart.com/aneer-engineers/) manufactured in India. Previous experience on generating such air-CO_2 reference mixture showed the effect of the regulator on determining analytical precision (Masarie *et al.* 2001; Allison *et al.* 2002). Routine analyses begin with a measurement of an aliquot (1 L) of air from the OASIS AIRMIX cylinder followed by analyses of the two flasks of air and terminate with an analysis of air from the OASIS AIRMIX cylinder. The procedure allows the determination of an external reproducibility based on pair values. The OASIS AIRMIX cylinder is also calibrated independently with the JRAS MAR-J1 and JRAS OMC-J1. The long term mean differences between the two measurements performed in a day on two samples of OASIS AIRMIX are 7 μmol·mol^{-1} for the mixing ratio and 0.05‰ for the $\delta^{13}C$ of CO_2 and these values are considered as the external reproducibility of air-CO_2 measurement for the internal air reference material as shown in figure 4 and mentioned in table 2. The overall long term reproducibility (standard deviation) of the absolute values measured for both the mixing ratio and the $\delta^{13}C$ of air-CO_2 from the OASIS AIRMIX cylinder showed a drift and the overall reproducibility is 12 μmol·mol^{-1} and 0.09‰, respectively and are explained in table 2. This value is established based on repeated processing and analysis of 418 air samples over a period of two years. The overall reproducibility observed is poor compared to the long term daily reproducibility between the duplicates. The role of the regulator, outlet valve and storage condition are probably the factors responsible for the poor long term reproducibility observed in our study (Allison *et al.* 2002; Toru and Kazuto 2003).

3. Atmospheric air-CO_2 measurement from Bangalore

Urban stations show large variability in the mixing ratio and the $\delta^{13}C$ of air-CO_2 (Demeny and Haszpra 2002; Pataki *et al.* 2003a; Affek *et al.* 2007; Newman *et al.* 2008) owing to factors like enhanced emission of anthropogenic CO_2, variation in source compositions, etc. Bangalore, being an urban location, is expected to capture similar changes in the isotopic composition and concentration of CO_2 in the air samples. The observed variability of the mixing ratio and the $\delta^{13}C$ in seasonal time scale (October 2008–December 2011) over Bangalore is quite large as mentioned in table 3. The average mixing ratio of CO_2 in seasonal time scale reaches its maxima (455 μmol·mol^{-1})

Table 3. *Mixing ratio and $\delta^{13}C$ of atmospheric CO_2 over an urban station Bangalore, India.*

Date	Mixing ratio ($\mu mol \cdot mol^{-1}$)	Difference in mixing ratio ($\mu mol \cdot mol^{-1}$)	$\delta^{13}C$ (‰ VPDB)	Difference in $\delta^{13}C$ (‰ VPDB)
26 January 2010	422		−8.34	
26 January 2010	437	14	−8.38	0.05
27 January 2010	425		−8.53	
27 January 2010	431	6	−8.40	0.13
2 February 2010	416		−8.52	
2 February 2010	420	3	−8.49	0.04
8 February 2010	466		−8.73	
8 February 2010	460	6	−8.70	0.04
9 February 2010	485		−8.87	
9 February 2010	485	0	−8.75	0.12
17 February 2010	474		−8.57	
17 February 2010	479	5	−8.58	0.01
18 February 2010	472		−8.61	
18 February 2010	466	6	−8.54	0.07
19 February 2010	460		−8.80	
19 February 2010	465	6	−8.76	0.04
20 February 2010	447		−8.46	
20 February 2010	447	0	−8.49	0.03
23 February 2010	460		−8.89	
23 February 2010	454	6	−8.87	0.02
24 February 2010	443		−8.72	
24 February 2010	447	4	−8.85	0.12
28 February 2010	454		−8.57	
28 February 2010	460	6	−8.62	0.05
2 March 2010	472		−8.64	
2 March 2010	472	0	−8.75	0.11
17 March 2010	472		−8.71	
17 March 2010	468	4	−8.69	0.02
30 March 2010	472		−8.76	
30 March 2010	472	0	−8.76	0.00
4 April 2010	472		−8.72	
4 April 2010	472	0	−8.84	0.11
9 April 2010	459		−8.80	
9 April 2010	469	10	−8.79	0.01
3 May 2010	444		−8.76	
3 May 2010	434	10	−8.87	0.11
31 May 2010	424		−8.59	
31 May 2010	424	0	−8.60	0.01
9 June 2010	409		−8.34	
9 June 2010	409	0	−8.29	0.04
13 June 2010	404		−8.32	
13 June 2010	404	0	−8.26	0.06
14 June 2010	409		−8.40	
14 June 2010	414	5	−8.35	0.05
16 June 2010	409		−8.53	
16 June 2010	409	0	−8.54	0.01
18 June 2010	404		−8.55	
18 June 2010	419	15	−8.50	0.05
22 June 2010	414		−8.60	
22 June 2010	414	0	−8.55	0.05
24 June 2010	424		−8.27	
24 June 2010	419	5	−8.32	0.05

Table 3. *(Continued)*

Date	Mixing ratio ($\mu mol \cdot mol^{-1}$)	Difference in mixing ratio ($\mu mol \cdot mol^{-1}$)	$\delta^{13}C$ (‰ VPDB)	Difference in $\delta^{13}C$ (‰ VPDB)
25 June 2010	420		−8.32	
25 June 2010	409	11	−8.31	0.01
28 June 2010	394		−8.39	
28 June 2010	399	5	−8.52	0.14
7 July 2010	422		−8.58	
7 July 2010	408	14	−8.46	0.11
16 July 2010	404		−8.18	
16 July 2010	414	10	−8.19	0.01
19 July 2010	414		−8.23	
19 July 2010	424	10	−8.30	0.06
21 July 2010	419		−8.17	
21 July 2010	419	0	−8.30	0.13
23 July 2010	427		−8.49	
23 July 2010	414	13	−8.41	0.09
28 July 2010	409		−8.42	
28 July 2010	404	5	−8.42	0.00
6 August 2010	414		−8.57	
6 August 2010	419	5	−8.56	0.01
9 August 2010	429		−8.46	
9 August 2010	434	5	−8.37	0.09
16 August 2010	444		−8.43	
16 August 2010	434	10	−8.45	0.02
18 August 2010	409		−8.48	
18 August 2010	394	15	−8.46	0.02
20 August 2010	436		−8.46	
20 August 2010	444	8	−8.50	0.03
3 September 2010	429		−8.24	
3 September 2010	436	7	−8.23	0.00
13 September 2010	422		−8.11	
13 September 2010	417	5	−8.17	0.06
20 September 2010	399		−8.32	
20 September 2010	404	5	−8.25	0.07
27 September 2010	404		−8.22	
27 September 2010	404	0	−8.17	0.05
29 September 2010	404		−8.21	
29 September 2010	409	5	−8.16	0.04
6 October 2010	434		−8.09	
6 October 2010	444	10	−8.09	0.01
20 October 2010	416		−8.18	
20 October 2010	419	3	−8.21	0.03
17 November 2010	404		−8.19	
17 November 2010	394	10	−8.05	
25 November 2010	409		−8.27	
25 November 2010	399	10	−8.31	0.04
29 November 2010	404		−8.23	
29 November 2010	393	11	−8.24	0.01
2 December 2010	414		−8.23	
2 December 2010	425	11	−8.31	0.08
8 December 2010	409		−8.24	
8 December 2010	420	11	−8.26	0.02
15 December 2010	412		−8.02	
15 December 2010	416	4	−8.06	0.04

Table 3. *(Continued)*

Date	Mixing ratio ($\mu mol \cdot mol^{-1}$)	Difference in mixing ratio ($\mu mol \cdot mol^{-1}$)	$\delta^{13}C$ (‰ VPDB)	Difference in $\delta^{13}C$ (‰ VPDB)
17 December 2010	429		−8.07	
17 December 2010	439	10	−8.11	0.04
20 December 2010	434		−8.23	
20 December 2010	444	10	−8.21	0.02
29 December 2010	419		−8.17	
29 December 2010	414	5	−8.31	0.13
3 January 2011	397		−8.17	
3 January 2011	397	0	−8.15	0.03
5 January 2011	407		−8.20	
5 January 2011	417	10	−8.24	0.04
12 January 2011	424		−8.40	
12 January 2011	439	15	−8.47	0.06
14 January 2011	428		−8.33	
14 January 2011	431	4	−8.31	0.02
19 January 2011	404		−8.39	
19 January 2011	417	13	−8.32	0.06
26 January 2011	414		−8.30	
26 January 2011	412	2	−8.38	0.09
31 January 2011	417		−8.26	
31 January 2011	429	11	−8.33	0.08
4 February 2011	424		−8.34	
4 February 2011	419	5	−8.41	0.07
3 March 2011	419		−8.54	
3 March 2011	424	5	−8.50	0.04
11 March 2011	449		−8.49	
11 March 2011	434	15	−8.50	0.01
16 March 2011	434		−8.64	
16 March 2011	439	5	−8.52	0.13
31 March 2011	443		−8.60	
31 March 2011	454	10	−8.71	0.10
5 April 2011	424		−8.42	
5 April 2011	439	15	−8.54	0.12
6 April 2011	428		−8.54	
6 April 2011	429	1	−8.56	0.02
7 April 2011	449		−8.54	
7 April 2011	459	10	−8.55	0.01
11 April 2011	439		−8.50	
11 April 2011	439	0	−8.48	0.02
20 April 2011	434		−8.56	
20 April 2011	439	5	−8.64	0.07
21 April 2011	435		−8.64	
21 April 2011	428	7	−8.77	0.13
25 April 2011	434		−8.54	
25 April 2011	449	15	−8.50	0.04
27 April 2011	424		−8.54	
27 April 2011	433	9	−8.64	0.10
29 April 2011	429		−8.58	
29 April 2011	434	5	−8.64	0.06
2 May 2011	424		−8.39	
2 May 2011	429	5	−8.49	0.10
6 May 2011	464		−8.50	
6 May 2011	454	10	−8.55	0.05

Table 3. *(Continued)*

Date	Mixing ratio ($\mu mol \cdot mol^{-1}$)	Difference in mixing ratio ($\mu mol \cdot mol^{-1}$)	$\delta^{13}C$ (‰ VPDB)	Difference in $\delta^{13}C$ (‰ VPDB)
11 May 2011	403		−8.24	
11 May 2011	408	5	−8.31	0.07
16 May 2011	459		−8.71	
16 May 2011	448	10	−8.82	0.11
20 May 2011	408		−8.43	
20 May 2011	424	15	−8.43	0.01
25 May 2011	424		−8.20	
25 May 2011	429	5	−8.31	0.11
27 May 2011	434		−8.22	
27 May 2011	427	7	−8.25	0.04
30 May 2011	412		−8.25	
30 May 2011	424	11	−8.24	0.02
3 June 2011	430		−8.37	
3 June 2011	427	3	−8.34	0.03
6 June 2011	434		−8.18	
6 June 2011	431	2	−8.28	0.10
8 June 2011	434		−8.25	
8 June 2011	418	15	−8.27	0.01
13 June 2011	418		−8.47	
13 June 2011	434	15	−8.35	0.12
15 June 2011	439		−8.23	
15 June 2011	439	0	−8.28	0.05
17 June 2011	425		−8.21	
17 June 2011	427	2	−8.26	0.05
20 June 2011	429		−8.27	
20 June 2011	436	7	−8.27	0.01
22 June 2011	424		−8.33	
22 June 2011	422	1	−8.38	0.05
24 June 2011	418		−8.26	
24 June 2011	413	6	−8.31	0.05
4 July 2011	407		−8.31	
4 July 2011	418	11	−8.34	0.03
6 July 2011	424		−8.41	
6 July 2011	424	0	−8.33	0.08
8 July 2011	408		−8.31	
8 July 2011	424	15	−8.30	0.01
11 July 2011	418		−8.20	
11 July 2011	408	10	−8.28	0.08
13 July 2011	412		−8.54	
13 July 2011	420	8	−8.46	0.08
15 July 2011	424		−8.31	
15 July 2011	408	15	−8.34	0.03
18 July 2011	407		−8.31	
18 July 2011	413	6	−8.38	0.08
21 July 2011	429		−8.50	
21 July 2011	413	15	−8.45	0.05
22 July 2011	402		−8.19	
22 July 2011	415	13	−8.25	0.06
25 July 2011	403		−8.38	
25 July 2011	402	1	−8.37	0.00
1 August 2011	449		−8.23	
1 August 2011	449	0	−8.29	0.06

Table 3. *(Continued)*

Date	Mixing ratio (µmol·mol^{-1})	Difference in mixing ratio (µmol·mol^{-1})	δ^{13}C (‰ VPDB)	Difference in δ^{13}C (‰ VPDB)
3 August 2011	413		−8.14	
3 August 2011	401	13	−8.16	0.02
5 August 2011	407		−8.27	
5 August 2011	407	0	−8.33	0.06
10 August 2011	424		−8.49	
10 August 2011	434	10	−8.45	0.04
23 August 2011	423		−8.11	
23 August 2011	424	1	−8.18	0.06
25 August 2011	449		−8.17	
25 August 2011	444	5	−8.21	0.05
2 September 2011	418		−8.09	
2 September 2011	434	15	−8.17	0.09
8 September 2011	424		−8.32	
8 September 2011	435	11	−8.46	
19 September 2011	439		−8.01	
19 September 2011	429	10	−8.08	0.07
28 September 2011	434		−8.00	
28 September 2011	444	10	−8.04	0.05
13 October 2011	434		−8.02	
13 October 2011	423	10	−7.99	0.03
20 October 2011	435		−8.01	
20 October 2011	441	6	−8.04	0.03
23 November 2011	412		−8.00	
23 November 2011	424	12	−8.05	0.05
24 November 2011	431		−7.99	
24 November 2011	429	1	−8.07	0.08
28 November 2011	414		−8.06	
28 November 2011	412	2	−8.12	0.06
20 December 2011	451		−8.32	
20 December 2011	448	3	−8.35	0.03
21 December 2011	448		−8.21	
21 December 2011	458	10	−8.30	0.09
External reproducibility (mean of differences)		7.0		0.05

during the dry hot summer months and minima (<419 µmol·mol^{-1}) during the time of southwest monsoon and post-monsoon season. Similarly, the average δ^{13}C values of atmospheric CO_2 reaches its minima (−8.80‰) during dry hot summer months and maxima (−8.14‰) during the post-monsoon months. The reproducibility of the atmospheric air-CO_2 measurement from Bangalore, India based on paired air samples collected at an elevation of 5 m above the ground; inside the IISc campus are 7 µmol·mol^{-1} and 0.05‰ for the mixing ratio and the δ^{13}C respectively as given in both tables 2 and 3. Thus, the reproducibility obtained for real air sample measurements for both the mixing ratio and the δ^{13}C of CO_2 matches closely with the reproducibility obtained for the paired analyses of the internal air reference mixture, OASIS AIR-MIX cylinder. The range of seasonal variation for both the mixing ratio and δ^{13}C of air-CO_2 reported here at the station is higher than the analytical reproducibility of the measurement.

3.1 *Response of local air-CO_2 to abrupt change in solar radiation during an annular solar eclipse on 15 January, 2010*

Events like a solar eclipse provide an opportunity to understand the response of the ecosystem to abrupt short term discontinuations in incoming solar radiation (Economou *et al.* 2008; Tominaga *et al.* 2010). The noontime annular solar eclipse on 15 January, 2010 was a unique event, being the longest eclipse of the millennium having a magnitude of 0.919 (Bhat and Jagannathan 2012). The trajectory of the eclipse over the Indian region is

Table 4. *Analytical results of air-CO_2 samples on the day of annular solar eclipse (15 January, 2010) and noneclipse.*

Sample ID	Event	Date	Time of sampling	Mixing ratio (μmol·mol^{-1})	δ^{13}C (‰ VPDB)
Air sample_S1	Eclipse day	15 January 2010	8.5	448	−8.59
Air sample_S2		15 January 2010	10.0	450	−8.60
Air sample_S3		15 January 2010	11.5	448	−8.55
Air sample_S4		15 January 2010	13.0	438	−8.41
Air sample_S5		15 January 2010	14.5	489	−11.00
Air sample_S6		15 January 2010	16.0	437	−8.43
Air sample_S7		15 January 2010	17.5	459	−8.91
Air sample_S8	Noneclipse day	25 January 2010	15.0	414	−8.36
Air sample_S9		25 January 2010	15.0	442	−8.52
Air sample_S10		26 January 2010	16.3	425	−8.54
Air sample_S11		26 January 2010	16.3	437	−8.33
Air sample_S12		26 January 2010	16.3	408	−8.35
Air sample_S13		26 January 2010	16.3	437	−8.39
Air sample_S14		27 January 2010	16.3	425	−8.55
Air sample_S15		27 January 2010	16.3	420	−8.35
Air sample_S16		27 January 2010	16.3	431	−8.41

well documented (Ratnam *et al.* 2010; Dutta *et al.* 2011; Bhat and Jagannathan 2012). In Bangalore, the eclipse began at 11:15 IST (Indian Standard Time), reached its peak at 13:22 IST and ended at 15:10 IST. The magnitude of the eclipse was 0.84 in Bangalore. Evidence of a drop in atmospheric temperature, wind speed, boundary layer height (Mishra *et al.* 2012) and photosynthetic activity (Ravi *et al.* 2010) were documented in several other studies. Since the atmospheric CO_2 is largely affected by photosynthetic activity (Pataki *et al.* 2003b) and boundary layer conditions (Guha and Ghosh 2010), it was interesting to record the atmospheric CO_2 concentration and isotope ratio during the solar eclipse. Air samples were collected from the top of a building within the campus of the Indian Institute of Science. The variation in the mixing ratio and the δ^{13}C of atmospheric CO_2 with time is presented in table 4 and shown in figure 5(a). The CO_2 mixing ratio increased by ∼50 μmol·mol^{-1}; with a corresponding depletion in the δ^{13}C value by ∼2‰, coinciding with the peak phase of the solar eclipse. A change of smaller magnitude in both concentration and isotope ratios in CO_2 was recorded in the air samples collected during the morning and afternoon from the same location in earlier studies (Guha and Ghosh 2010). Factors like a night time inversion layer in drawing high concentrations and depleted isotopic signatures were suggested. We also analyzed air samples on other days in the same months following the day of the eclipse, mainly during the afternoon to characterize the anomalous isotopic composition and mixing ratio observed during the event (figure 5a). A change in concentration and isotope ratios during the peak time of the solar eclipse can be explained by a lowering of the atmospheric boundary layer (Mishra *et al.* 2012). The lowering of the atmospheric boundary layer might allow the capturing of CO_2 at the ground level. A Keeling two-component model approach is used to identify the composition of CO_2 in an end member source of air (figure 5b). The δ^{13}C composition of the end member is −32.9‰ as characterized by the sample collected during the eclipse, indicating the presence of CO_2 from fossil fuel combustion. This δ^{13}C intercept is abnormally depleted compared to our earlier observations on end member compositions during the morning and afternoon samples collected during the winter at our sampling site (Guha and Ghosh 2010). An abrupt change in the isotopic composition of source air-CO_2 particularly on the day of the eclipse can be explained by the inversion layer mediated trapping of CO_2 at the ground level. This concentration and isotopic effect seen is significantly large and possibly indicates the capture of CO_2 emissions coinciding with the peak hour of emissions in Bangalore (Bathmanabhan and Madanayak 2010). The study is the first of its kind where the lowering of the boundary layer mimicked night time conditions promoting trapping of more locally produced CO_2 at the ground level.

4. Summary

An experimental set-up was prepared for measuring the mixing ratio and δ^{13}C of atmospheric CO_2. The internal precision obtained for the δ^{13}C of atmospheric CO_2 is ±0.03‰, based on a repeat analysis of the same sample. The set-up has been

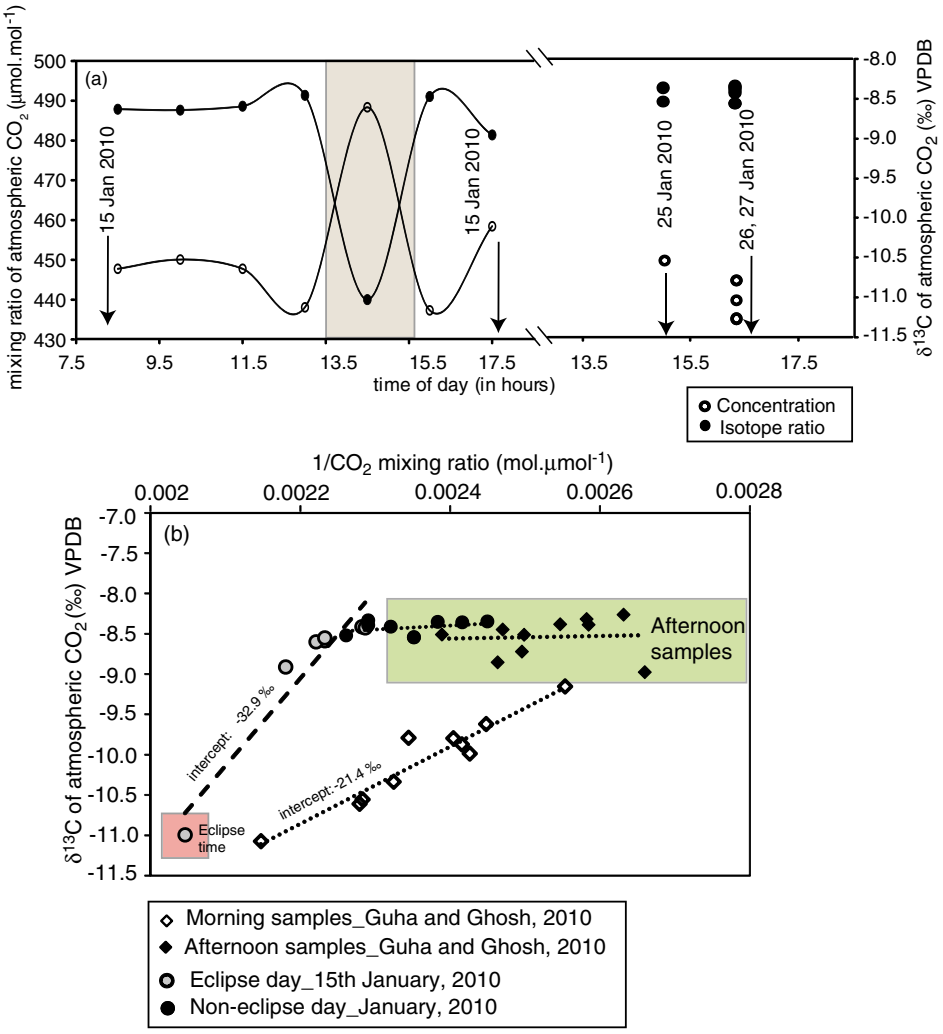

Figure 5. (**a**) Variation of mixing ratio (left axis) and δ^{13}C of air-CO_2 (right axis) observed in air samples collected from the sampling station inside Indian Institute of Science campus on the day of annular solar eclipse on 15 January, 2010 and other days in the same month. (**b**) A plot between the inverse of the mixing ratios and δ^{13}C value of air-CO_2 in morning time and afternoon time air samples. A drastic change in the end member composition from −21.4‰ observed in morning samples compared to −32.9‰ observed during the eclipse day is highlighted. Green shaded region with enriched δ^{13}C values of air-CO_2 demarcate the composition of afternoon time air samples, while red zone marks the afternoon sample collected on the day of eclipse.

used to measure the atmospheric CO_2 mixing ratio and carbon isotope ratio in the air over Bangalore for the last two years. The set-up is capable of delivering a reproducibility of ±7 µmol·mol^{-1} and ±0.05‰ for the paired measurement of both air samples and cylinder air for the mixing ratio and the δ^{13}C of CO_2 from the air samples. However, long term reproducibility in cylinder air is 12.4 µmol·mol^{-1} and 0.09‰ for the mixing ratio and the δ^{13}C of CO_2. We measured the variation of the CO_2 mixing ratio and isotope ratio observed in the air samples from Bangalore during the annular solar eclipse event on 15 January, 2010. The eclipse provided an opportunity to capture the effect of the lowering of the boundary layer in trapping locally produced CO_2 at the ground level (figure 5).

Acknowledgements

The authors would like to thank Dr Willi Brand and his research group at MPI for the two flasks of the JRAS reference tank. This manuscript is a contribution to the Ministry of Earth Science, Government of India, project MoES/ATMOS/PP-IX/09. They also thank the Divecha Centre for Climate Change, IISc for financial support and the Department of Science and Technology for funding the OASIS AIRMIX cylinder and IAEA standards. A special thanks to Prof. J S Srinivasan, Divecha Centre for Climate Change, IISc for supporting the activity and Dr R Chakrabarti for proofreading. They extend special thanks to the anonymous reviewers for their constructive comments and suggestions.

References

Affek H P and Eiler J M 2006 Abundance of mass 47 CO_2 in urban air, car exhaust, and human breath; *Geochim. Cosmochim. Acta* **70** 1–12.

Affek H P, Xu X and Eiler J M 2007 Seasonal and diurnal variations of $^{13}C^{18}O^{16}O$ in air: Initial observations from Pasadena, CA; *Geochim. Cosmochim. Acta* **70** 1–12.

Allison C E, Francey R J and Steele L P 2002 The International Atomic Energy Agency Circulation of Laboratory Air Standards for Stable Isotope Comparisons: Aims, Preparation and Preliminary Results; In: *Isotope aided studies of atmospheric carbon dioxide and other greenhouse gases – Phase II* (IAEA-TECDOC-1269), IAEA, Vienna, Austria, pp. 5–23.

Assonov S S and Brenninkmeijer C A M 2006 On the N_2O correction used for mass spectrometric analysis of atmospheric CO_2; *Rapid Commun. Mass Spectrom.* **20** 1809.

Bathmanabhan S and Madanayak S N S 2010 Analysis and interpretation of particulate matter – PM10, PM2.5 and PM1 emissions from the heterogeneous traffic near an urban roadway; *Atmos. Pollution Res.* **1** 184–194.

Bhat G S and Jagannathan R 2012 Moisture depletion in the surface layer in response to an annular solar eclipse; *J. Atmos. Sol. Terr. Phys.* **80** 60–67.

Coplen T B 1996 New guidelines for reporting stable hydrogen, carbon, and oxygen isotope-ratio data; *Geochim. Cosmochim. Acta* **60(17)** 3359–3360.

Craig H 1953 The geochemistry of the stable carbon isotopes; *Geochim. Cosmochim. Acta.* **3** 53.

Craig H and Keeling C D 1963 The effect of atmospheric N_2O on the measured isotopic composition of atmospheric CO_2; *Geochim. Cosmochim. Acta* **27** 549.

Demeny A and Haszpra L 2002 Stable isotope compositions of CO_2 in background air and at polluted sites in Hungary; *Rapid Commun. Mass Spectrom.* **16** 797–804.

Dutta G, Kumar P V, Ratnam M V, Mohammad S, Kumar M C A, Rao P V, Rahaman K and Basha H A 2011 Response of tropical lower atmosphere to annular solar eclipse of 15 January, 2010; *J. Atmos. Sol. Terr. Phys.* **73** 1907–1914.

Economou G, Christou E D, Giannakourou A, Gerasopoulos A, Georgopoulos D, Kotoulas V, Lyra D, Tsakalis N, Tzortziou M, Vahamidis P, Papathanassiou E and Karamanos A 2008 Eclipse effects on field crops and marine zooplankton: The 29 March 2006 total solar eclipse; *Atmos. Chem. Phys.* **8** 4665–4676.

Francey R J, Steele L P, Langenfelds R L, Lucarelli M P, Allison C E, Breadsmore D J, Coram S A, Derek N, de Silva F R, Etheridge D M, Fraser P J, Henry R J, Turner B, Welch E D, Spencer D A and Cooper L N 1996 Global Atmospheric Sampling Laboratory (GASLAB): Supporting and extending the Cape Grim trace gas programs; In: *Baseline Atmospheric Program Australia (Austaria) 1993* (eds) Francey R J, Dick A L and Derek N, Department of the Environment, Sport and Territories, Bureau of Meteorology in Cooperation with CSIRO Division of Atmospheric Research, Melbourne, pp. 8–29.

Ghosh P and Brand W A 2004 The effect of N_2O on the isotopic composition of air-CO_2 samples; *Rapid Comm. Mass Spectrom.* **18** 1830.

Ghosh P, Patecki M, Rothe M and Brand W A 2005 Calcite-CO_2 mixed into CO_2-free air: A new CO_2-in-air stable isotope reference material for the VPDB Scale; *Rapid Comm. Mass Spectrom.* **19** 1097.

Guha T and Ghosh P 2010 Diurnal variation of atmospheric CO_2 concentration and $\delta^{13}C$ in an urban atmosphere during winter – role of the Nocturnal Boundary Layer; *J. Atmos. Chem.* **65** 1–12, doi: 10.1007/s10874-010-9178-6.

Hoefs J 1995 *Stable isotope geochemistry*, Springer, Germany.

Keeling C D 1958 The concentration and isotopic abundance of carbon dioxide in rural areas; *Geochim. Cosmochim. Acta* **13** 322–334.

Laurila T 2007 14th WMO/IAEA meeting of experts on carbon dioxide, other greenhouse gases and related tracers measurement techniques; GAW Report no. 186.

Masarie K A, Langenfelds R L, Allison C E, Conway T J, Dlugokencky E J, Francey R J, Novelli P C, Steel L P, Tans P P, Vaughn R and White J M C 2001 NOAA/CSIRO flask air intercomparison experiment: A strategy for directly assessing consistency among atmospheric measurements made by independent laboratories; *J. Geophys. Res.* **106(D17)** 20445–20464.

McCrea J M 1950 The isotopic chemistry of carbonates and a paleo-temperature scale; *J. Chem. Phys.* **18** 849–857.

Mishra M K, Rajeev K, Nair A K M, Krishnamoorthy K and Parameswaran K 2012 Impact of a noon-time annular solar eclipse on the mixing layer height and vertical distribution of aerosols in the atmospheric boundary layer; *J. Atmos. Sol. Terr. Phys.* **74** 232–237.

Mook W G and Groots P M 1973 The measuring procedure and corrections for the high-precision mass-spectrometric analysis of isotopic abundance ratios, especially referring to carbon, oxygen and nitrogen; *Int J. Mass Spectrom. Ion Phys.* **12** 273–298.

Mook W G and Hoek S V 1983 The N_2O correction in the carbon and oxygen isotopic analysis of atmospheric CO_2; *Isotope Geosci.* **1** 237.

Newman S, Xu X, Affek H P, Stopler E and Epstein S 2008 Changes in mixing ratio and isotopic composition of CO_2 in urban air from the Los Angeles basin, California, between 1972 and 2003; *J. Geophys. Res.* **113(D23304)**, doi: 10.1029/2008JD009999.

Pataki D E, Bowling D R and Ehleringer J R 2003a Seasonal cycle of carbon dioxide and its isotopic composition in an urban atmosphere: Anthropogenic and biogenic effects; *J. Geophys. Res.* **108(D23)** 4735, doi: 10.1029/2003JD003865.

Pataki D E, Ehleringer J R, Flanagan L B, Yakir D, Bowling D R, Still C J, Buchmann N, Kaplan J O and Berry J A 2003b The application and interpretation of Keeling plots in terrestrial carbon cycle research; *Global Biogeochem. Cycles* **17(1)** 1022, doi: 10.1029/2001GB001850.

Ratnam M V, Kumar M S, Basha G, Anandan V K and Jayaraman A 2010 Effect of the annular solar eclipse of 15 January 2010 on the lower atmospheric boundary layer over a tropical rural station; *J. Atmos. Sol. Terr. Phys.* **72** 1393–1400.

Ravi V, George J, Latha R, Murthy B S, Dharamaraj T, Ravindran C S and Naskar S K 2010 Effect of the annular solar eclipse of 15 January 2010 on meteorological variables, photosynthetic electron transport rate and photosystem II efficiency of Cassava (*Manihot esculenta* Crantz.); *J. Root Croops* **36(1)** 72–77.

Santrock J, Studley S A and Hays J M 1985 Isotopic analyses based on the mass spectra of carbon dioxide; *Analytical Chemistry* **57(7)** 1444–1448.

Stichler W 1995 Interlaboratory comparison of new materials for carbon and oxygen isotope ratio measurements; In: *Reference and intercomparison materials for stable isotopes of light elements*, Proceedings of a consultants meeting, Vienna (IAEA-TECDOC, 825). Vienna, Austria, International Atomic Energy Agency, pp. 67–74.

Tans P P, Fung I Y and Takahashi T 1990 Observational constraints on the global atmospheric CO_2; *Science* **247** 1431–1438, doi: 10.1126/science.247.4949.1431.

Tominaga J, Kawasaki S, Yabuta S, Fukuzawa Y, Suwa R and Kawamitsu Y 2010 Eclipse effects on CO_2 profile within and above Sorghum Canopy; *Plant Prod. Sci.* **13(4)** 338–346.

Toru S and Kazuto S 2003 Report of the 11th WMO/IAEA Meeting of Experts on Carbon Dioxide Concentration and Related Tracer Measurement Techniques; GAW report no. 184.

Wendeberg M, Richter J M, Rothe M and Brand W A 2011 $\delta^{18}O$ anchoring to VPDB: Calcite digestion with ^{18}O-adjusted ortho-phosphoric acid; *Rapid Comm. Mass Spectrom.* **25** 851–860.

Werner R A, Rothe M and Brand W A 2001 Extraction of CO_2 from air samples for isotopic analysis and limits to ultra high precision $\delta^{18}O$ determination in CO_2 gas; *Rapid Comm. Mass Spectrom.* **15** 2152.

MS received 24 July 2012; revised 13 December 2012; accepted 17 December 2012